International Journal of Orthopaedics

Online Submissions: http://www.ghrnet.org/index.php/ijo
doi:10.17554/j.issn.2311-5106.2018.05.240

Int. J. of Orth. 2018 February 28; 5(1): 883-890
ISSN 2311-5106 (Print), ISSN 2313-1462 (Online)

ORIGINAL ARTICLE

A Novel MRI Measurement for Analysing Coracoacromial Morphology

Kadosa Bodo, Mustafa Abbas, David Temperley FRCR, Prof Adrian Midgley PhD, Puneet Monga FRCS (Tr&Orth)

Kadosa Bodo, Mustafa Abbas, Clinical Research Fellow (2014), Department of Orthopaedic Surgery, Wrightington Wigan and Leigh, NHS Trust, Hall Lane, Wigan, WN6 9EP, UK
David Temperley, Consultant Radiologist, Department of Radiology, Wrightington Wigan and Leigh, NHS Trust, Hall Lane, Wigan, WN6 9EP, UK
Adrian Midgley, Professor of Exercise Physiology, Department of Sport & Physical Activity, Faculty of Arts and Sciences, Edge Hill University, St Helens Road, Ormskirk, Lancashire, L39 4QP, UK
Puneet Monga, Consultant Orthopaedic Surgeon, Department of Orthopaedic Surgery, Wrightington Wigan and Leigh, NHS Trust, Hall Lane, Wigan, WN6 9EP, UK

Conflict-of-interest statement: The author(s) declare(s) that there is no conflict of interest regarding the publication of this paper.

Correspondence to: Kadosa Bodo, Clinical Research Fellow (2014), Department of Orthopaedic Surgery, Wrightington Wigan and Leigh, NHS Trust, Hall Lane, Wigan, WN6 9EP, UK
Email: bokadi71@gmail.com
Telephone: +44(0)1942 244000

Received: October 1, 2017
Revised: December 20, 2017
Accepted: December 22 2017
Published online: February 28, 2018

ABSTRACT

AIMS: Extrinsic factors of subacromial impingement of the shoulder can be potentially characterised by the angle between the acromion and coracoacromial ligament. A retrospective study was designed to test a novel angle measurement method for a potential new diagnostic tool.

PATIENTS AND METHODS: The landmarks and outcome measures were determined on sagittal cuts of default 1.5 T MRI scans. Two independent observers made the measurements on 50 annotated images of a cohort of healthy and young individuals.

RESULTS: The mean acromial-coracoacromial ligament (ACAL) angle was 129.8 degrees, (SD 10.0). The two independent measurements and a repeated one were compared for testing inter- and intra-observer reliability. Measurement of ACAL showed high internal consistency and strong measurement agreement between observers (Cronbach's alpha values: 0.88, 0.86 and 0.94; Intraclass correlation coefficient values: 0.78, 0.75, 0.88). However, a statistically significant difference (p=0.035) was found on the retest measurement (1st to 2nd) of the same observer, despite the little difference (1st to 3rd $p = 0.78$; 2nd to 3rd $p = 0.75$) in inter-observer relation on paired sample t-test.

CONCLUSIONS: The measuring error came from poor definition of the landmarks on standard 3 mm slice thickness MRI scans. Altered scanning sequences with thinner slices might provide more details of the structures, improve reliability, and prove to be a clinically useful measure in a future prospective study.

KEY MESSAGES: ACAL measurement was not sufficiently reliable when performed on a default plane MRI scan; however, an altered scanning method might provide better visualisation and higher definition of the structures and could improve intra-observer reliability in further studies.

Key words: Arch, coracoacromial; Ligament; Angle; Subacromial; Impingement

Bodo K B, Abbas M E, Temperley D, Midgley A W, Monga P. A Novel MRI Measurement for Analysing Coracoacromial Morphology. *International Journal of Orthopaedics* 2018; **5(1)**: 883-890 Available from: URL: http: //www.ghrnet.org/index.php/ijo/article/view/2150

Legend

ACAL: acromion-coracoacromial ligament angle; *CAL*: coracoacromial ligament length; *Acrm*: Acromion length; *Hypot*: Hypotenuse length; *Glen*: Glenoid supero-inferior diameter; spur:

acromial spur in mm; Acrm shape: acromial morphology according to Bigliani and Vanarthos and Monu classification; *SSP outlet*: supraspinatus outlet area; *Normalised*: the SSP outlet area/glenoid height

INTRODUCTION

Impingement syndrome is a common cause of shoulder pain with an annual incidence of between 0.9 and 2.5% and with a lifetime prevalence from 6.9% to 66.7% in the general population worldwide[1]. Shoulder pain was the third most common musculoskeletal condition reported in primary care in 2005 and about 1% of the adult population presented with new onset shoulder pain. The majority (70%) of them related to rotator cuff pathology[2].

With the advent of magnetic resonance imaging, it is now possible to examine soft tissue changes and to define the three-dimensional anatomy of the coracoacromial arch without using radiation. Several studies found magnetic resonance imaging (MRI) scans to be reliable, sensitive and specific to detect rotator cuff tears and impingement-related changes, such as the distortion of the coracoacromial arch[3-4]. The coracoacromial arch anatomy on MRI has been described and various studies published with comparisons of differences in the subacromial space on MRI between symptomatic and asymptomatic cohorts[5-8]. Most of the studies required computerised analysis and, therefore, are not reproducible in everyday clinical settings, unlike the acromial-coracoacromial ligament (ACAL) angle, which has potential for routine clinical use. This present study explored the use of MRI scans to identify extrinsic causes of subacromial impingement, which might potentially serve as a diagnostic tool for shoulder impingement and aid surgical decision making. Additionally, this feature would potentially provide further details for understanding the pathogenesis of shoulder impingement syndrome and rotator cuff disease. This study aimed to quantify the anatomical appearance of the coracoacromial arch on MRI scans via measurements using recognisable landmarks.

METHODS AND MATERIALS

This specific measurement method has not been published previously and owing to its novelty the precise technique was defined and its inter- and intra-observer reliability were determined during this study. Sample size was calculated using a prospective power calculation. A similar previously published study was used as an example. Roidis *et al*. (2009) measured the supraspinatus outlet area on MRI scans in two cohorts of patients[8]. The mean outlet area was 577 mm^2 in asymptomatic young patients and 481 mm^2 in rotator cuff deficient adults. The mean difference of 96 mm^2 was significant, (p = 0.036). Using the frequencies of the above publication, a Chi-square table was constructed by an independent statistician and it was found that 50 patients were required in each arm of the study to obtain statistical power of 80% at an alpha value of 0.05. Measurements were then taken on 50 annotated, previously performed MRI images from the archive of the Hospital's Radiology Department. The study used asymptomatic and rotator cuff deficient cohorts of patients to meet the original aims of the research. No patient identifiable data was used and no patients were physically involved in the study. For confidentiality purposes, the images were annotated, and were listed and identified by their unique hospital 7-digit PAS number (Patient Administration System, NHS IT Framework), which was unrelated and unlinked to any other identifiable data. The list and images were stored in a separate encrypted file in the radiology department's PC for further reference until the study was completed and then it was deleted. This file was accessible only to the research team members. The study was registered at the hospital's research and development department and via the Integrated Research Application System (IRAS). Favourable ethical opinion was given by the Health Research Authority's East of England National Research Ethics Service (NRES) Committee (Project ID 127015, REC reference 14/EE/0047). The study conformed to the ethical principles outlined in the Declaration of Helsinki.

MRI scan images were produced by two 1.5 Tesla scanners, Phillips Intera Archieva and Siemens Aera, in the Radiology Department of the Trust. The images were then uploaded and stored in the Picture Archiving and Communication System (PACS). This software was also used for the measurements (Centricity Enterprise TM, GE Healthcare Ltd) and is a popular clinical tool in assessing radiological images[9]. The researchers aimed to formulate this new measurement method for use in everyday clinical practice and this warranted testing on PACS, which by default provided all the necessary electronic measuring tools, for example, angle and distance measurements. Hence, the researchers believed that testing the method in a real clinical situation added extra value to the study. The study was performed on standard hospital PCs (Dell GX755 Desktop PC 17' LCD Monitor).

In order to reduce the confounding factor of ageing, young patients' preoperative annotated MRI scans (between 18-25 years of age, with an average age of 22 years) were used for this phase of the study, hypothesising that the coracoacromial arch would lack degenerative changes. The images, obtained between 09/10/2012 and 30/09/2013, were quasi-randomly selected from the hospital's Radiology Department database according to date of birth and orthopaedic history in the radiology reports. The most common indication for the MRI scan was shoulder instability and the majority of the scans were MRI arthrograms. The authors stipulated that the ACAL angle should not be affected by the small amount of intra-articular contrast agent (gadolinium). Sixty-two images were selected, irrespective of gender, race, dexterity, occupation, area of living, social circumstances, recreation or sport activity, health or co-morbidities. By gender, 50 male and 12 female patients' MRI scans were collected with an approximate sex ratio of 4:1. Males were over-represented in the sample compared to the previously published ratio of 1.8:1[10]. The high male/female ratio could be explained by the high incidence of sport injuries in the catchment area where rugby was popular. In order to reduce other confounding factors, certain conditions were excluded, such as fracture, septic arthritis, tumour, previous acromioplasty, previous rotator cuff reconstruction, or other surgery that had left an implant in the area of interest.

According to inclusion and exclusion criteria 62 shoulder MRI scans were selected, comprising 10 plain MRI scans and 52 MRI arthrograms. Twenty scans were excluded: five had fractures, four were poor quality, seven had previous surgery, two had os acromiale and two scans were not accessible. Five additional MRI scans were available that had been performed on the contra-lateral shoulders of the same patients and three more from two patients who had repeated MRI scans on the same joint in various years. In addition, eight more available image-sets were included resulting in a total of 50 MRI scans collected for the study. To reduce ascertainment bias, the measurements were carried out blind and independently by two clinical research fellows (Observer A and B) who were an experienced orthopaedic trainee and trained orthopaedic surgeon, respectively. Both were familiar with the PACS software. Observer B repeated the measurements on all 50 MRI scans after a 2-week washout period. This washout period was used to reduce recall bias. The 50 MRI scans were then reviewed three times by the two observers: observer “B” did the first (M1) and second (M2) repeated measurements and observer “A” did the third (M3) counter-measurement.

The ACAL angle was established and defined among well recognised bony landmarks and the line of the coracoacromial ligament (CAL) on T2 weight sagittal MRI scan images, specifically on cuts where the coracoid tip just appeared (Figure 1 and Figure 2). The vertex of the angle was on the anterior margin of the acromion where the CAL was inserted. The anterior side was along the CAL and ended at the ligament’s origin on the coracoid process. The posterior side was drawn along the under-surface of the acromion and ended at its posterior end. Then the two sides were connected with a line forming a triangle and were used as the hypotenuse. In order to test the measurement reliability, secondary outcome measures were established. The length of the sides (CAL and acromion) and the hypotenuse, and the territory of the triangle were calculated. The latter was believed to correspond to the supraspinatus outlet area[8]. It was then normalised with glenoid height in order to adjust the values to an individual basis. Glenoid height was believed to correspond to the patients’ overall body characteristics and it was defined as its supero-inferior diameter, a distance between the base of the coracoid at the proximal pole and the base of the scapular wing at the distal pole of the glenoid rim. When acromial spurs were observed, their extensions from the acromial plane were measured at a right angle (Figure 1b). These measurements provided continuous data for further statistical analysis. The observed acromia were classified according to Bigliani’s concept[11]. The following categories were used: type I, as flat; type II, as curved; and type III, as hooked shaped in cross section. For describing a convex shaped acromion, a type IV category was used according to Vanarthos and Monu classification[12]. A plan was made to conduct another study using participants with symptomatic shoulders and then acromial configuration would have been relevant, hence the rationale for distinguishing acromia type. These categorical data were collected in order to complete the analysis with previously stipulated features of impingement[13-14].

Figure 1 a+b: Examples for ACAL angle measurement. The landmarks: undersurface of acromion, the coraco-acromial ligament and its acromial and coracoid attachments, and the posterior edge of acromion. These points form a triangle, representing an area of a cross section of the subacromial space.

Figure 2 a+b: The ACAL angle measurement landmarks on plain x-ray and sagittal MRI scan image of the same shoulder joint. It is noticeable the plane of the sagittal MRI slice cuts through the ligament in an angle as it represented with the purple line. It may explain the ligament segmental appearance on the image.

Altogether 150 measurements were taken and 8 outcome measures were collected each time. The three sets of measurements were then compared for inter-observer and intra-observer reliability. For the statistical analysis IBM®SPSS® Statistics Version 22 software was used (SPSS Inc., Chicago, IL). Distribution, maximum and minimum values of the range, the mean with a 95% confidence interval and standard deviation (SD) of each outcome were calculated using descriptive statistical analysis. Relative reliability was calculated using the intraclass correlation coefficient (ICC) and Cronbach’s Alpha. Absolute reliability was calculated with a paired samples t-test. The paired sample correlation, mean difference, standard deviation of the differences (diff SD), standard error of the mean difference (SEM), and p value were calculated. Statistically significant changes were accepted at $p < 0.05$. Cronbach’s alpha was considered as acceptable between 0.60-0.69, good if between 0.70-0.89 and excellent if above 0.90. The ICC was interpreted as moderate agreement between 0.50-0.69, strong agreement between 0.70-0.79, and almost perfect agreement above 0.80[15-16].

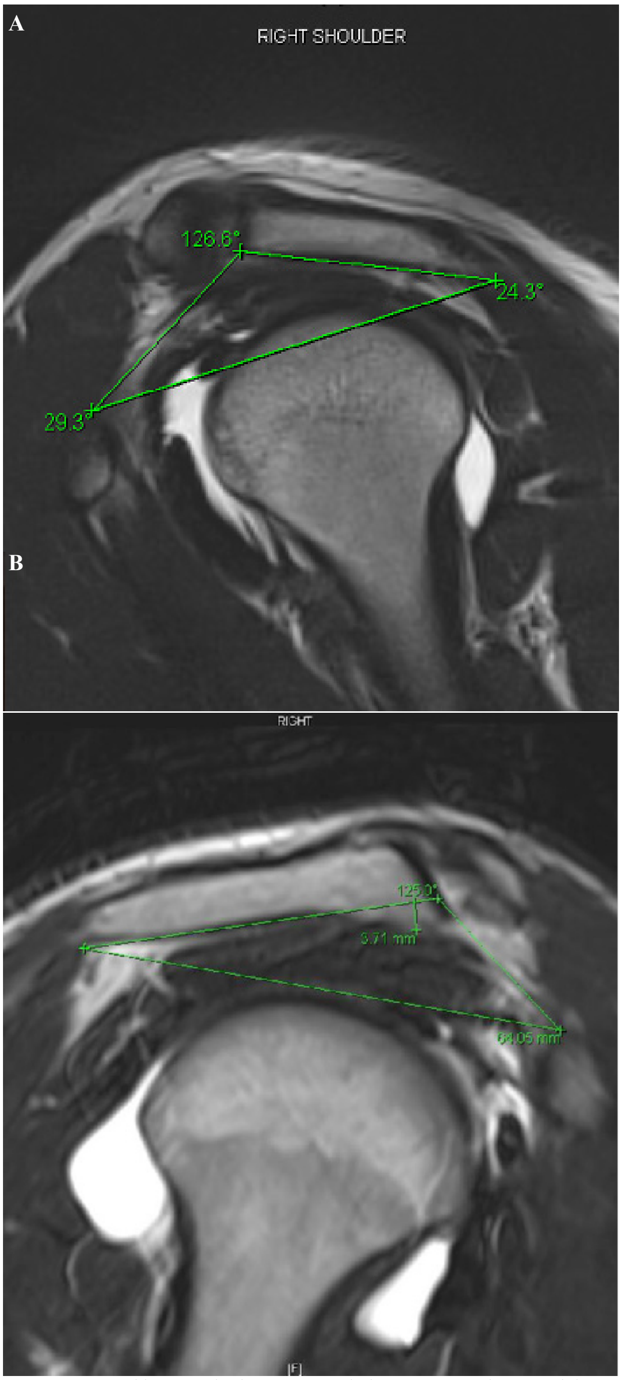

Figure 1 A: In this example the ACAL angle is 126.6°. **B:** The acromial spur extension is measured in right angle to its undersurface.

RESULTS

The mean ACAL angle was 129.7° (95% CI = 128.5° – 131.7°; SD 10.03). The range was from 105.6° to 154.9° and the distribution was Gaussian. Comparing the ACAL angle measurements (M1 to M3; M2 to M3; M1 to M2) showed high internal consistency (Cronbach’s alpha 0.88, 0.86 and 0.94) and strong measurement agreement (ICC of 0.78, 0.75, and 0.88). Despite the high correlations, the

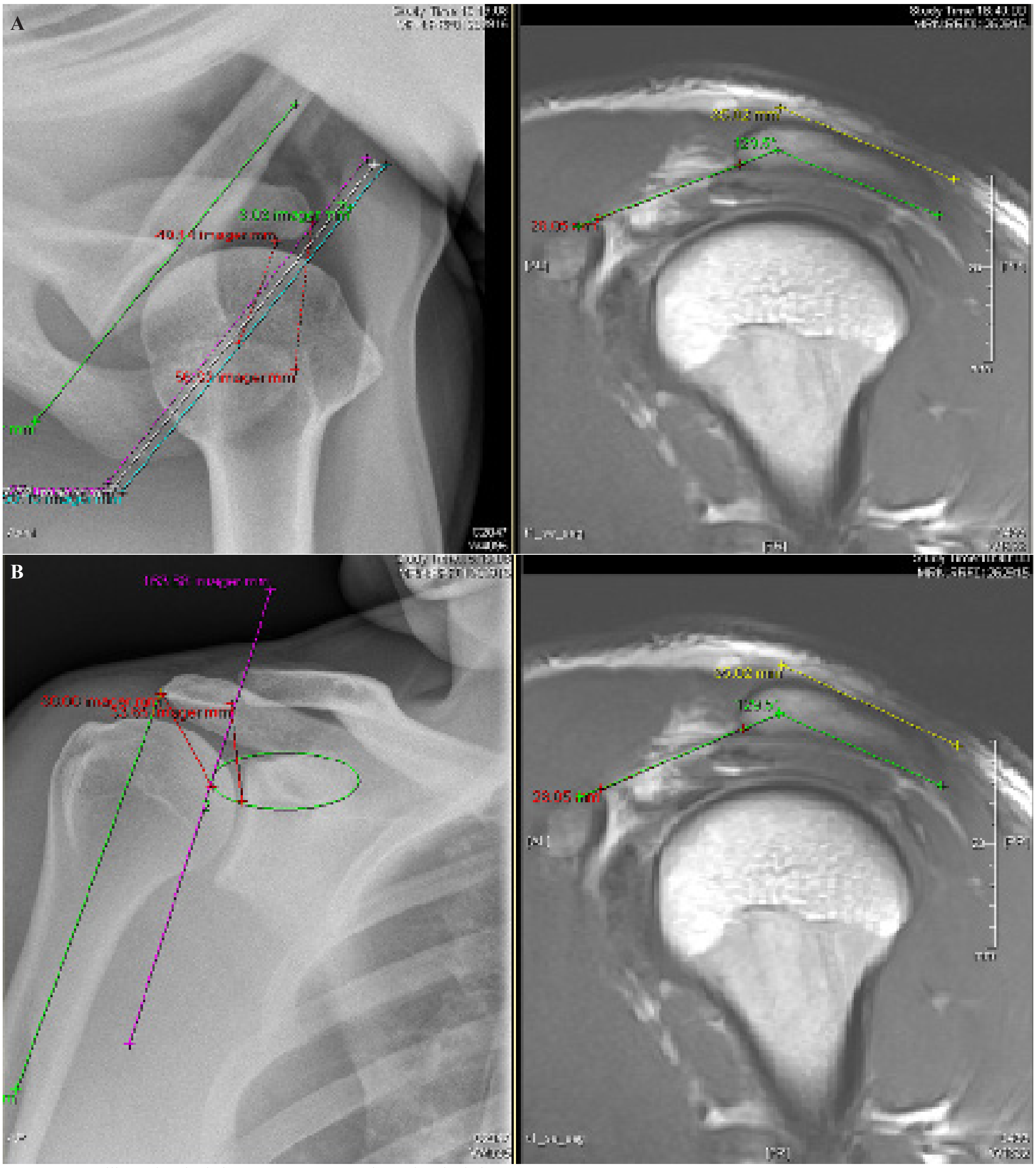

Figure 2 A: Axillar and sagittal views; **B:** Antero-posterior and sagittal views

paired sample analysis showed a significant mean difference (*p* = 0.035) in the measured angles when comparing the first (M1) and repeated (M2) measurements, indicating systematic bias across repeated measures. The measured angles were closer together (*p* = 0.15 and *p* = 0.91) in the inter-observer relations, namely the first to third and second to third measurements, which were reliable. Scatter plots (Graph 1, Graph 2, Graph 3) demonstrated a good relative relationship among the arms, but systematic error of the measurements. Bland-Altman plots (Graph 4, Graph 5, Graph 6) were generated and all three plots showed symmetric and wide distribution, with no particular pattern, suggesting no systematic bias, but systematic error of measurements as confidence intervals were in a wide range.

The paired mean differences were only a few degrees (M1 *vs* M3 1.38°, M2 *vs* M3 0.11°, M1 *vs* M2 1.5°) and the range of the differences for the paired angles was from 0.1° to 20.6°. The SD of the differences were 4.8° (M1 *vs* M2), 6.7° (M1 *vs* M3) and 7.1° (M2 *vs* M3) and it was expected the difference between the measurements of two different observers would be within the range of +/- 1.96 SD, namely from 9.4° to 13.9° and there was 95% chance for two separate measurements would differ by +/- 12.1°. The Bland-Altman plots showed the level of agreement was too wide a range (+/- 12.1°) for measuring potentially less than 10° pathological alteration on the MRI scans in spite of the very little difference between the means of the measurements. The secondary outcome measures were less reliably measured, as some of them had poor correlations and others had significant mean differences across measurements (Table 1).

DISCUSSION

The main aim of the present study was to develop a novel measuring method for the coracoacromial arch on standard MRI scans of the shoulder and test its intra- and inter-observer reliability. Two observers measured the angle of the acromion to the coracoacromial ligament (ACAL angle) along with other secondary measures. The ACAL angle might have been unrelated to the actual size of the ligament, the acromion or the coracoid process, and as the ligament is connected to two fixed points of the bony scapula, it was considered as constant. It appeared to be well measurable and the mean difference among the measured angle values was statistically non-significant between observers, but significant across the repeated measurements of observer B. The systematic error might have been from various causes.

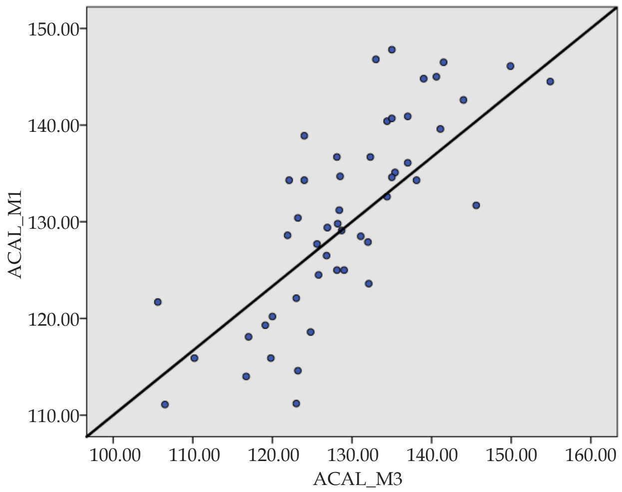

Graph 1 Scatter plot representing inter-observer correlation.

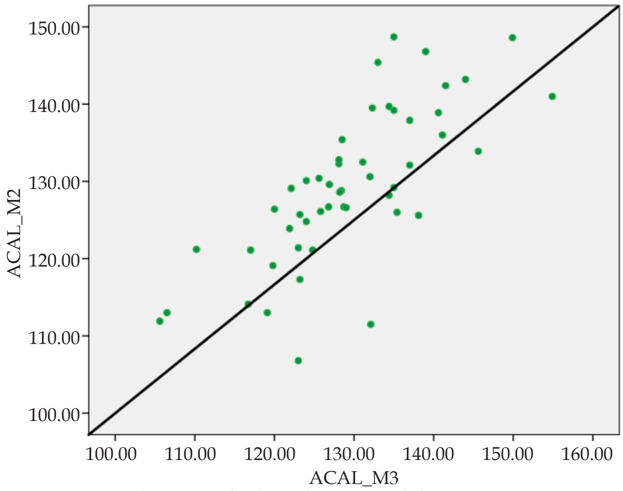

Graph 2 Scatter plot representing inter-observer correlation.

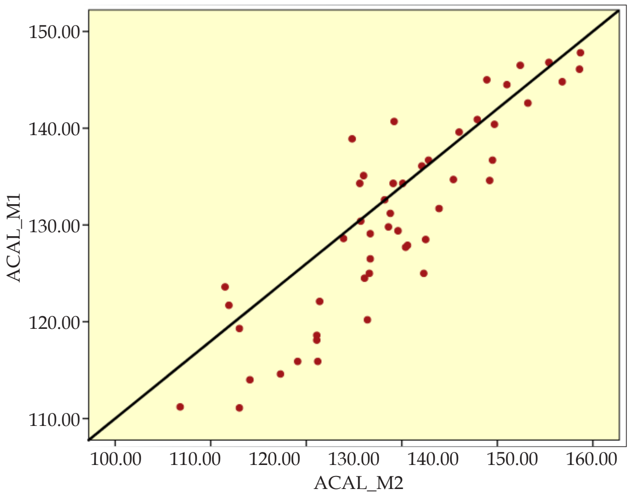

Graph 3 Scatter plot representing intra-observer correlation.

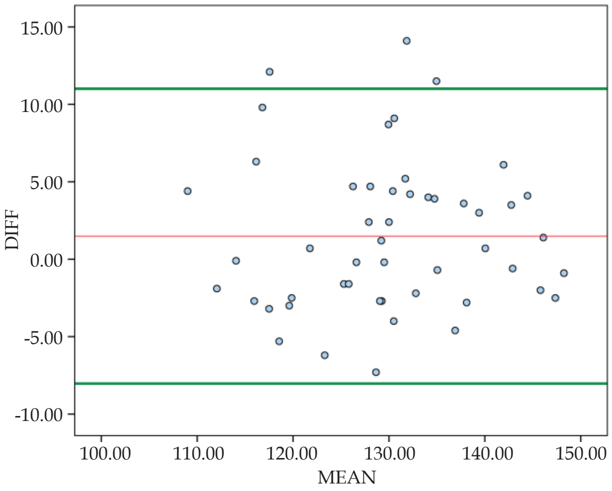

Graph 4 Bland-Altman Plot of ACAL angle M1 and M2 with Mean Diff 1.5° 95%CI -8.026° – 11.01° (intra-observer reliability).

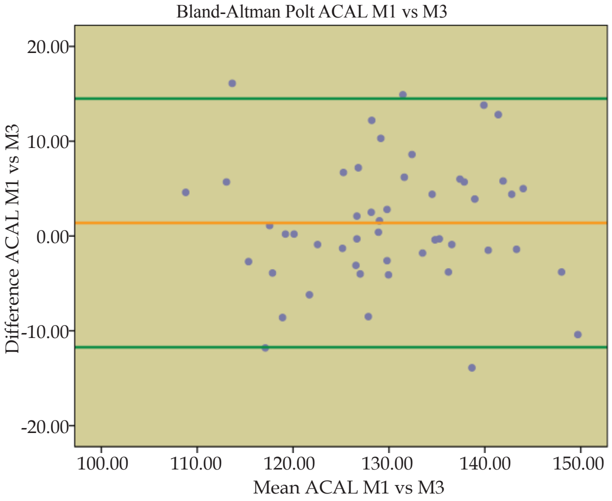
Bland-Altman Polt ACAL M1 vs M3

Graph 5 Bland-Altman Plot of ACAL angle M1 vs M3 measurement with Mean Diff 1.38° 95% CI -11.75°- 14.5° (inter-observer reliability).

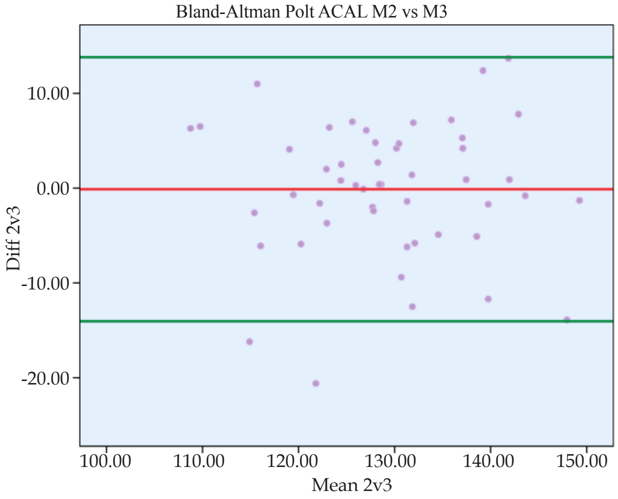
Bland-Altman Polt ACAL M2 vs M3

Graph 6 Bland-Altman Plot of ACAL angle M2 vs M3 measurement with Mean Diff -0.11° 95% CI -14.3°-13.8° (inter-observer reliability).

Firstly, the angle and distances were measured on a computer screen using the same software that is widely used for clinical purposes for radiological images assessment and analysis, although the measurements were operator dependent. It was believed if the method worked in those circumstances then clinical applicability would have been possible straight away. As the method did not differ from everyday clinical practice, no further training was required. The software provided in-built validated distance and angle measurement tools and, regardless of its validity, the measurements were different due to possible human factors.

Secondly, the measured angles and distances were based on the end-points and their positions were limited by the pixel grid, the crosshair could have been on particular pixels only, compromising the measurement, but more importantly, the bony landmarks definition was not always sufficient to precisely set the points. Greater magnification was associated with lower definition as the images became pixelated. Furthermore, it was difficult to define the under surface of the acromion, especially when it was uneven, such as in convex (type IV) or curved (type II) acromial morphology. Additionally, it was observed that the acromion cross-section changed shaped on each cut, some appeared to be type III, type II, or even type I depending on the actual cut. The type III appearance was seen on only one slice of the sets in several cases. The authors agreed to draw the line under the acromion that best matched its overall plane most of the time, but this practice might explain the statistically significant measurement error. The line cut off the hooked part of the acromion (type III) forming a reference line for the hook measurement. The hook measurement showed large variability because of a few millimetres difference on the screen which was practically unnoticeable owing to the measuring tool's relative line and end-point thickness.

Table 1 Summarised reliability test results. Green fields are representing the intra-observer reliability results. White fields are inter-observer results. Outlying results are highlighted with red.

	Relative Reliability			**Absolute Reliability**	
Measure	**Cronbach's Alpha**	**Intraclass Correlation Coefficient (ICC)**	**ICC Sig**	**t-test Paired Samples Correlations**	**t-test 2-tailed Sig**
ACAL M1M3	0.876	0.78	0	0.78	0.152
ACAL M2M3	0.857	0.749	0	0.749	0.91
ACAL M1M2	0.939	0.884	0	0.884	0.035
CAL M1M3	0.683	0.519	0	0.519	0.888
CAL M2M3	0.898	0.815	0	0.818	0.04
CAL M1M2	0.777	0.635	0	0.639	0.19
Acrm M1M3	0.893	0.807	0	0.815	0
Acrm M2M3	0.9	0.819	0	0.819	0.043
Acrm M1M2	0.907	0.83	0	0.837	0.028
Hypot M1M3	0.889	0.8	0	0.813	0
Hypot M2M3	0.928	0.866	0	0.874	0
Hypot M1M2	0.941	0.888	0	0.889	0.336
Glen M1M3	0.694	0.531	0	0.538	0
Glen M2M3	0.88	0.785	0	0.785	0.578
Glen M1M2	0.814	0.686	0	0.697	0
Spur M1M3	0.414	0.261	0.032	0.267	0.152
Spur M2M3	0.803	0.671	0	0.671	0.326
Spur M1M2	0.736	0.582	0	0.593	0.32
Acrm Shape M1M3	0.451	0.291	0.019	0.293	0.696
Acrm Shape M2M3	0.679	0.514	0	0.515	0.811
Acrm Shape M1M2	0.777	0.635	0	0.635	0.792
SSP Outlet M1M3	0.798	0.664	0	0.672	0.006
SSP Outlet M2M3	0.824	0.701	0	0.712	0.015
SSP Outlet M1M2	0.916	0.845	0	0.845	0.432
Normalised M1M3	0.725	0.569	0	0.572	0.69
Normalised M2M3	0.774	0.632	0	0.634	0.023
Normalised M1M2	0.858	0.751	0	0.764	0.002

Thirdly, with the naked eye a 5 degrees difference was unnoticeable and even these small variations could have brought statistically significant differences in the measured values. This drawback of the measuring tool might have been rectified by magnification but in return the over-enlargement made the border of the measurable structures pixelated and they became blurred on the screen. It could be considered as a major disadvantage of the usage of MRI scan images compared to high definition plain radiographs, but even x-ray measurement has been reported to be controversial[9]. Additionally, a well-defined measuring method, such as the Cobb angle for scoliosis, has been reported as unreliable in the case of premature skeletons due to poor visualisation of bony landmarks on the radiograph[17]. However, with the evolution of radiological imaging in the future, it might be possible to use the same method with a better outcome. Apparently, these tools at present could only be used as an estimate in everyday clinical practice. In return, using another more reliable piece of software and tools would take away practicality and would only add value for research purposes, which would not meet the research team's original aims. It is possible that more detailed training and feedback for the measurement method would have provided a better outcome. However, to test the method's reproducibility from a simulation that would be reasonably practicable in clinical practice, the simple measurements were performed after a description of the method and a short discussion and agreement of the process of identifying specific landmarks. A future study could be repeated in modified circumstances, for example, with the use of three-dimensional reconstruction and a computer-aided measuring assistance tool. The available MRI scans for this present research had 3 mm slice thickness and good quality 3-D reconstruction was not possible. However, a future study could be designed with thinner sliced scans, for example 1 mm, which would provide far more detail. The image definition can be improved by using stronger MRI scanners[18-19]. The study could be repeated with 3 Tesla instead of 1.5 Tesla magnetic field strength using a scanner, which might significantly increase the image quality as shown in other studies[20-21]. However, consideration should be taken because longer scanning times might increase motion artefacts and a stronger scan could decrease the signal-to-noise ratio. An altered plane sagittal scan might provide better visualisation (Figure 3a and Figure 3b). However, this would require repeating the scans by reconstructing the images from available MRI scans; which is possible, but the digital rendering would potentially lead to an inferior definition of the structures, therefore producing pixelated and blurred images. The sagittal-oblique plane scan would cut the ligament in its full length and would provide a sagittal cut of the acromion at the level of the presumed impingement. It also might help the visualisation of the acromial morphology as it would provide a cross-section of the acromion at the insertion point of the ligament at the acromial tip. It would lead to a more reliable agreement in the classification and would also help to establish the measuring line at the under-surface of the acromion, which was one of the limitations of the present study.

The exact role of CAL is still not clear and is debated in the literature. The ligament's own mechanoreceptors and deformation of the ligament on dynamic ultrasound scan are reported, which suggests its function as a restraint and also with a role in proprioception[22]. It is also reported the ligament can reform or regenerate after surgical transection, suggesting its functional importance as an anatomical structure[23-24]. The altered plane MRI scan may reveal further morphological features to aid understanding of the role of CAL in impingement.

Figure 3 a+b: The desired plane of sagittal MRI scan visualising the coraco-acromial arch, including the full length of CAL and cross section of the acromion.

Figure 3 A: sagittal-oblique plane along the aspect of CAL (orange marking). Please note the angle between the glenoid (blue line) and the modified plane (green line); B: The sagittal oblique plane along the aspect of CAL (orange marking). Please note the angle of the modified plane (green line) to the glenoid (blue line).

CONCLUSION

Measurement of the angle of the ligament to the acromion (ACAL angle) was hypothesised to be relevant so that a steeper angle decreases the subacromial space, leading to increased contact and pressure of the above-mentioned structures. Even though the ACAL angle was measured with good correlation between the observers, within the first and repeated observations the measured values were significantly different. An altered scanning method might provide better visualisation and higher definition of the structures and could improve intra-observer reliability in further studies.

ACKNOWLEDGEMENTS

The authors acknowledge the assistance of Karen Emery (PACS Manager), and Lindsay Cunningham (Radiographer) for their help with this study to access Radiology Department database at Wrightington Hospital and of Sandra Latham (Research and Development Administrator) for her help in Research Ethical Committee's process. The authors acknowledge the assistance of Kanthan Theivendran BSc(Hons), MBBS, MRCS, FRCS (Tr & Orth) for his help in reviewing the manuscript. The authors acknowledge the assistance of David Nuttall (independent statistician) for his help in power calculation.

REFERENCES

1. Luime JJ, Koes BW, Hendriksen IJ, Burdorf A, Verhagen AP, Miedema HS, *et al*. Prevalence and incidence of shoulder pain in the general population; a systematic review. *Scand J Rheumatol*. 2004; **33**: 73-81. [PMID: 15163107]
2. Mitchell C, Adebajo A, Hay E, Carr A. Shoulder pain: Diagnosis and management in primary care. *BMJ*. 2005; **331**: 1124-8. [PMID: 16282408]; [DOI 10.1136/bmj.331.7525.1124]
3. Kaneko K, DeMouy EH, Brunet ME. MR evaluation of rotator cuff impingement: Correlation with confirmed full-thickness rotator cuff tears. *J Comput Assist Tomogr*. 1994; **18**: 225-8. [PMID: 8126271]
4. Tan RK. A review of the role of magnetic resonance imaging in the evaluation of shoulder impingement syndrome and rotator cuff tendon tears. *Annals of the Academy of Medicine*. 1998; **27**: 243-7. [PMID: 9663318]
5. Farley TE, Neumann CH, Steinbach LS, Petersen SA. The coracoacromial arch: MR evaluation and correlation with rotator cuff pathology. *Skeletal Radiol*. 1994; **23**: 641-5. [PMID: 7886475]
6. Gold GE, Pappas GP, Blemker SS, Whalen ST, Campbell G, McAdams TA, *et al*. Abduction and external rotation in shoulder impingement: An open MR study on healthy volunteers initial experience. *Radiology*. 2007; **244**: 815-22. [PMID: 17690321]; [DOI 10.1148/radiol.2443060998]
7. Graichen H, Bonel H, Stammberger T, Haubner M, Rohrer H, Englmeier KH, *et al*. Three-dimensional analysis of the width

of the subacromial space in healthy subjects and patients with impingement syndrome. *AJR Am J Roentgenol*. 1999; **172**: 1081-6. [PMID: 10587151]; [DOI: 10.2214/ajr.172.4.10587151]

8. Roidis NT, Motamed S, Vaishnav S, Ebramzadeh E, Karachalios TS, Itamura JM. The influence of the acromioclavicular joint degeneration on supraspinatus outlet impingement and the acromion shape. *J Orthop Surg (Hong Kong)*. 2009; **17**: 331-4. [PMID: 20065375]; [DOI: 10.1177/230949900901700318]
9. Wilson JD, Eardley W, Odak S, Jennings A. To what degree is digital imaging reliable? validation of femoral neck shaft angle measurement in the era of picture archiving and communication systems. *Br J Radiol*. 2011; **84**: 375-9. [PMID: 21159801]; [DOI: 10.1259/bjr/29690721]
10. te Slaa RL, Wijffels MP, Brand R, Marti RK. The prognosis following acute primary glenohumeral dislocation. *J Bone Joint Surg Br*. 2004; **86**: 58-64. [PMID: 14765867]
11. Bigliani LU, Morrison DS, April EW. The morphology of the acromion and its relationship to rotator cuff tears. *Orthop. Trans*. 1986; **10**: 228.
12. Vanarthos WJ, Monu JU. Type 4 acromion: A new classification. *Contemp Orthop*. 1995; **30**: 227-9. [PMID: 10150316]
13. Epstein RE, Schweitzer ME, Frieman BG, Fenlin JM,Jr, Mitchell DG. Hooked acromion: Prevalence on MR images of painful shoulders. *Radiology*. 1993; **187**: 479-81. [PMID: 8475294]; [DOI: 10.1148/radiology.187.2.8475294]
14. Nicholson GP, Goodman DA, Flatow EL, Bigliani LU. The acromion: Morphologic condition and age-related changes. A study of 420 scapulas. *J Shoulder Elbow Surg*. 1996; **5**: 1-11. [PMID: 8919436]
15. Lee KM, Lee J, Chung CY, Ahn S, Sung KH, Kim TW, *et al*. Pitfalls and important issues in testing reliability using intraclass correlation coefficients in orthopaedic research. *Clin Orthop Surg*. 2012; **4**: 149-55. [PMID: 22662301]; [DOI: 10.4055/cios.2012.4.2.149]
16. Portney LG, Watkins MP. Chapter 26: Statistical Measures of Reliability. In: Watkins MP, editor. Foundations of clinical research: Applications to practice, 2nd ed. New Jersey, United States: Prentice Hall Inc.; 2000. p. 560-567.
17. Modi HN, Chen T, Suh SW, Mehta S, Srinivasalu S, Yang JH, *et al*. Observer reliability between juvenile and adolescent idiopathic scoliosis in measurement of stable cobb's angle. *Eur Spine J*. 2009; **18**: 52-8. [PMID: 19037669]; [DOI: 10.1007/s00586-008-0834-3]
18. Loew R, Kreitner KF, Runkel M, Zoellner J, Thelen M. MR arthrography of the shoulder: Comparison of low-field (0.2 T) *vs* high-field (1.5 T) imaging. *Eur Radiol*. 2000; **10**: 989-96. [PMID: 10879716]; [DOI: 10.1007/s003300051050]
19. Magee T, Shapiro M, Williams D. Comparison of high-field-strength versus low-field-strength MRI of the shoulder. *AJR Am J Roentgenol*. 2003; **181**: 1211-5. [PMID: 14573405]; [DOI: 10.2214/ajr.181.5.1811211]
20. Gibbs GF, Huston J,3rd, Bernstein MA, Riederer SJ, Brown RD, Jr. Improved image quality of intracranial aneurysms: 3.0-T versus 1.5-T time-of-flight MR angiography. *AJNR Am J Neuroradiol*. 2004; **25**: 84-7. [PMID: 14729534]
21. Gutberlet M, Schwinge K, Freyhardt P, Spors B, Grothoff M, Denecke T, *et al*. Influence of high magnetic field strengths and parallel acquisition strategies on image quality in cardiac 2D CINE magnetic resonance imaging: Comparison of 1.5 T vs. 3.0 T. *Eur Radiol*. 2005; **15**: 1586-97. [PMID: 15875193]; [DOI: 10.1007/s00330-005-2768-z]
22. Rothenberg A, Gasbarro G, Chlebeck J, Lin A. The Coracoacromial Ligament: Anatomy, Function, and Clinical Significance. *Orthop J Sports Med*. 2017; **5**: 1-8. [PMID: 28508008]; [DOI: 10.1177/2325967117703398]
23. Levy O, Copeland SA. Regeneration of the coracoacromial ligament after acromioplasty and arthroscopic subacromial decompression. *J Shoulder Elbow Surgery*. 2001; **10**: 317-320. [PMID: 11517360]; [DOI: 10.1067/mse.2001.116519]
24. Bak K, Spring BJ, Henderson IJ. Re-formation of the coracoacromial ligament after open resection or arthroscopic release. *J Shoulder Elbow Surgery*. 2000; **9**: 289-293. [PMID: 10979523]; [DOI 10.1067/mse.2000.106318]

Peer Reviewers: Stig Brorson; Rubén Arellano